GEOPHYSICAL RESEARCH LETTERS, VOL. 17, NO. 5, PAGES 599-602, APRIL 1990

RAPID WHISTLER-MODE WAVE GROWTH RESULTING FROM FREQUENCY-TIME CURVATURE

R. A. Helliwell, T. Mielke, and U. S. Inan

STAR Laboratory, Stanford University

Abstract. The rapid (<50 ms) temporal growth of ducted whistlers is simulated using controlled injection of VLF pulses from the Siple Station, Antarctica transmitter. The results show that, when the frequency- time function of the injected pulse has a positive slope and negative curvature, producing a kind of "chirp" such that it approximates the $f(t)$ shape of a lightning-generated whistler at frequencies above the 'nose' frequency, growth up to a saturation level (20-30 dB) commonly occurs within <50 ms as opposed to 200-300 ms that is required for monochromatic input signals. The phenomenon is explained in terms of second-order-resonance theory [*Helliwell*, 1967; *Carlson et al.*, 1985; *Chang et al.*, 1983] where the frequency variation of the pulse matches the changing cold plasma parameters, facilitating enhanced resonance interactions over extended portions of the field line.

Magnetospheric whistler-mode signals that originate in ground sources (e.g. lightning, VLF transmitters) often stimulate or trigger nonlinear responses in the form of amplified signals, narrowband variable frequency emissions and complex sidebands [*Helliwell*, 1988]. One such effect commonly associated with nose whistlers is the growth of the whistler in the upper part (above the 'nose') of its frequency range and the associated emission triggering that tends to occur at the whistler's upper cutoff frequency (usually at 0.5 f_H, where f_H is the equatorial electron gyrofrequency). An example of the dynamic spectrum of such an event is shown in Figure 1*a* where the growth of the whistler is represented by the darkening and broadening of the upper segment of the trace. The whistler triggered emission is, in essence, a narrowband oscillation of slowly-varying center frequency. What makes this phenomenon remarkable is the relatively short time (~50 ms) of growth (~20dB) of the whistler compared with the time (200-400 ms) required for a monochromatic signal under comparable conditions to exhibit the same growth [*Helliwell*, 1988]. Since the triggered emissions associated with whistlers and constant frequency signals (such as those from VLF transmitters) are comparable in their intensities (as observed on the ground or on satellites) and spectral characteristics, one might expect the mechanisms of their generation to be the same. On the other hand, since the typical peak intensities of whistlers excited by lightning impulses are likely to exceed the signal level injected from ground-based transmitters that have been used in such experiments, one might simply attribute the observed difference in behavior to unknown nonlinear effects (none is suggested here) related to the high intensity of the input signals. In this paper, we describe a new experiment where the upper part (i.e. frequencies above the nose frequency [*Helliwell*, 1965]) of a one-hop nose whistler is simulated using the Siple Station experimental VLF transmitter [*Helliwell*, 1988] to reproduce two-hop nose whistlers that may exhibit the rapid growth described above (e.g. Figure 1*a*).

Paper number 90GL00524
0094-8276/90/90GL-00524$03.00

1. Description of the Experiment

The Stanford University VLF wave-injection experiments employ a VLF transmitter at Siple Station, Antarctica, and receivers at Roberval and Lake Mistissini, Quebec (50°N, 74°W. Both are near the conjugate point to Siple Station.) [*Helliwell*, 1988]. For the experiment described herein a test wave form was designed by fitting the frequencies in a train of contiguous 1 ms segments (above the nose frequency) to a model of one-hop whistlers similar to those shown in Figure 1*b*. The resulting pulse was then injected from Siple as a simulated 1-hop whistler, which at Lake Mistissini resembles a 2- hop whistler. The results are illustrated by the spectra in Figures 1*c*, and 1*d*. Both growth and emission triggering are stimulated by the nose whistler simulation (NOWS) which can therefore be said to have reproduced the principal features of amplified natural nose whistlers. A further demonstration of the enhanced growth rate of NOWS signals is shown in Figure 2 in which the spectra and amplitude profiles of the responses to a representative NOWS signal and a continuous wave (cw) signal of about the same input power are compared. Here we see that the saturation level is about the same (-5dB) for both signals, but the peak growth rates are ≈ 1250 dB/s for NOWS and 55dB/s (a typical value) for the CW reference signal. Thus the effective NOWS growth rate is ≈ 20 times the CW rate. It should be noted that the transmitted CW reference signal was ramped up in amplitude at a rate of 10 dB/s. This power ramp was intended to aid in measuring the threshold level below which temporal amplification does not occur [*Helliwell et al.*, 1980; *Helliwell*, 1988]. In this instance, the observed CW growth rate (55 dB/s) greatly exceeds 10dB/s from the start of the pulse, showing that the CW input signal power was always above the threshold for CW growth. Once the triggering threshold is reached the temporal growth rate tends to be independent of subsequent increases in the intensity of the input signal. Hence a correction for the 10 dB/s amplitude ramp is not required when measuring the temporal growth rate.

From the results illustrated in Figures 1 & 2, we conclude that a pulse of the appropriate $f(t)$ curvature grows much faster than a CW signal at any frequency within the NOWS signal range. It is interesting therefore to pack NOWS pulses as close together in time as possible in order

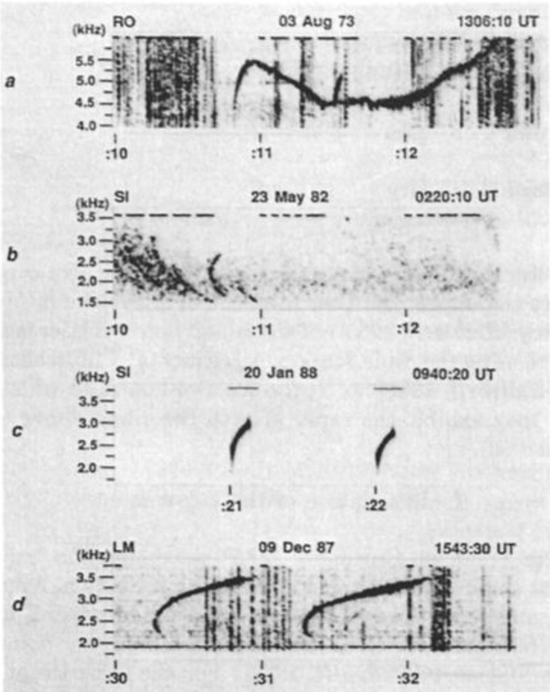

Fig. 1. Natural and artificial nose whistlers. (a) two-hop whistler with triggered emissions observed at Roberval, Canada; (b) one-hop whistlers observed at Siple Station, Antarctia; (c) NOWS (NOse Whistler Simulation) test waveform to simulate one-hop whistler; (d) growth and emissions observed on NOWS signals at Lake Mistissini, Canada.

to enhance the averaged wave power output that would be associated with the higher growth rate of a NOWS pulse. The spectrum of such a composite signal, which we shall refer to as a 'NOWS cluster', is shown in Figure 3a, and consists of an unbroken sequence of similar NOWS pulses whose frequency ranges are decreased in steps of 16 Hz and where the center frequencies simultaneously are decreased in steps of 70 Hz. The signal spectrum as received at Lake Mistissini is shown in Figure 3b, along with its rms amplitude in Figure 3c (filter bandwidth=1 kHz). Each NOWS pulse shows growth followed by a triggered emission that tends to entrain the next emission, forming an irregular emission band at the upper border of the cluster. Several independent triggered emissions are also seen on each cluster, primarily on the first 4 or 5 NOWS pulses. Panels d, e, and f show the same type of data from a diagnostic signal sequence, consisting of stepped CW pulses and frequency ramps, a 2-sec amplitude ramp, and a frequency doublet (two equal amplitude carriers spaced 20 Hz apart). As can be seen by comparing the NOWS cluster with the diagnostic sequence, the average NOWS level is -4 dB, whereas the maximum level for the diagnostic pulses is about -8 dB, a gain of 4 dB for the NOWS format. The 1st element of the second cluster of NOWS pulses even reaches 0 dB, suggesting that "fine tuning" of the NOWS format might produce nearly a factor of 10 increase in average signal power extracted from the magnetosphere compared with a CW input, thus enhancing particle precipitation.

The occurrence of NOWS growth and triggering has to date always been associated with CW pulse growth. For all recordings on which no CW pulse growth was seen,

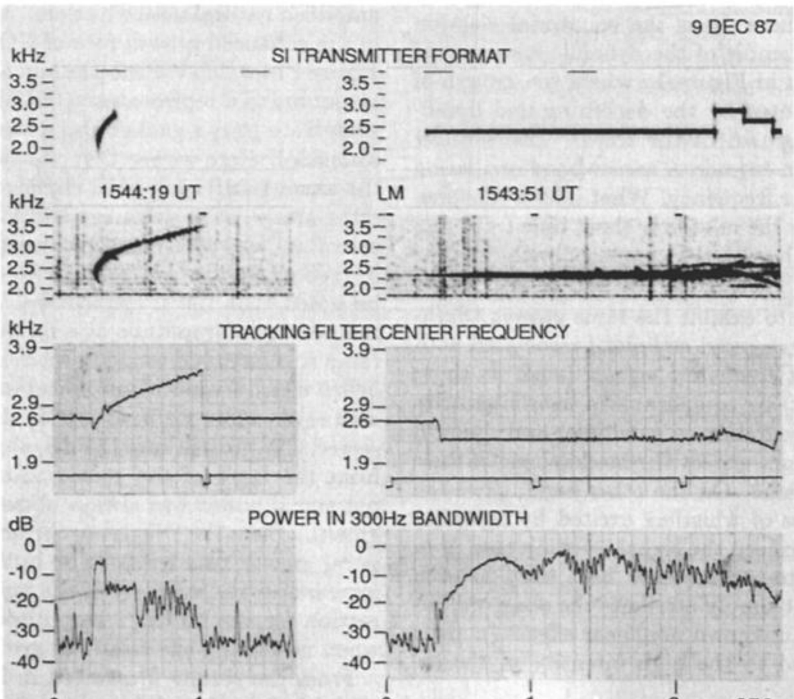

Fig. 2. Simulated nose whistler (left hand column) and constant frequency pulse (right hand column).

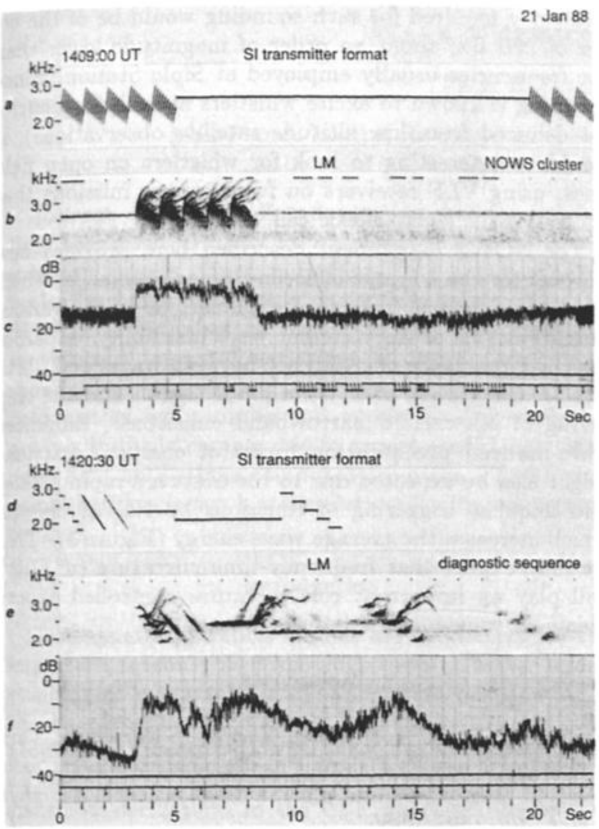

Fig. 3. NOWS cluster and diagnostic sequence. Panels *c* and *f* show power in a 1 kHz bandwidth centered at 2.64 kHz.

there were no traces of the NOWS format. In the present study the NOWS format was observed at Lake Mistissini on sixty-one occasions between 25 July 1986 and 20 January 1987 and between 30 November 1987 and 21 January 1988. The NOWS signal sequences were only detectable in 70% of the cases in which the CW signal showed growth. In about 20% of those cases the artificial nose whistler was visible but showed no growth, while in 50% of the cases the artificial nose whistler was detected and showed growth. Thus the simulated nose whistler was about half as effective as a CW pulse in causing growth. Quantitative details of NOWS occurence statistics and growth patterns will be reported later.

2. Interpretation

To explain the results reported above we invoke the concept of second order resonance [*Helliwell*, 1967, 1970; *Carlson et al.*, 1985], which, in essence, results in a spatial extension of the region of doppler-shifted cyclotron resonance which is believed to be the basis for spontaneous and triggered VLF emissions. Simply stated, second order resonance occurs where the spatial variations of the doppler-shifted wave frequency, $\omega' = \omega + kv_{\parallel}$, and the electron gyrofrequency ω_H are matched. For given spatial variations of wave frequency ω, wave number k, gyrofrequency ω_H, plasma frequency ω_N and electron parallel velocity $v_{\parallel}$, a region can be found where the duration of resonance between an electron and the wave train is a maximum. Since this location depends on the local rate of change of the wave frequency (df/dt) [*Helliwell*, 1970; *Carlson, et al.*, 1985], different parts of the NOWS wave train will exhibit second order resonance at different locations along the propagation path.

This situation is illustrated by the sketch in Figure 4, where the curved NOWS trace is approximated by three straight line segments each of which corresponds to second order resonance with electrons at the location shown. Each of these linear segments is amplified through feedback in much the same way as a CW wave is amplified on the equator [*Helliwell*, 1970; *Helliwell and Inan*, 1982]. However, because of the curvature of f(t), a wave segment with a particular slope does not last long enough for the signal to reach saturation at that location. Instead growth occurs only while there is significant phase bunching. Thus each slope corresponds to extended resonance

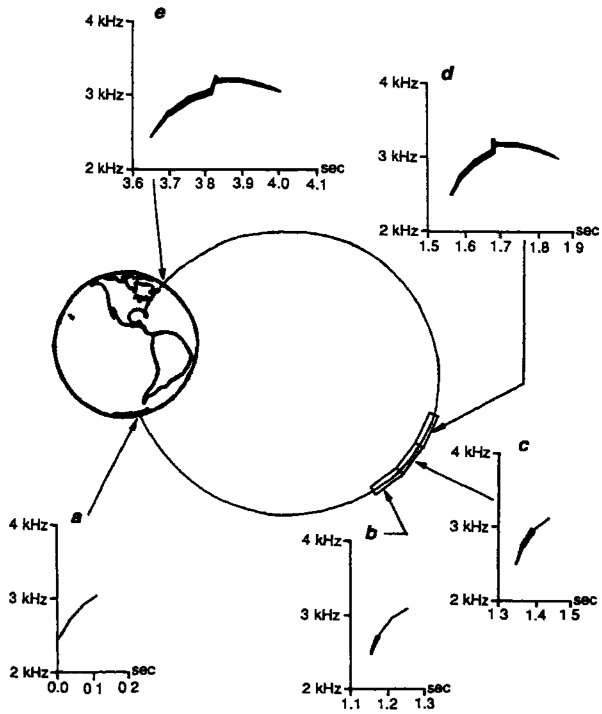

Fig. 4. Schematic of the NOWS interaction. (*a*) an approximation to a one-hop whistler is transmitted from Siple Station, Antarctica. The actual parabolic curve of frequency versus time is represented here as three straight-line segments; (*b*) the initial segment, with the lowest frequency and steepest slope is resonant farthest from the equator. Some growth occurs; (*c*) the intermediate frequency and slope segment is resonant on an adjacent region of the magnetic field line. Further growth occurs, aided by the enhanced wave power entering the resonant region; (*d*) the highest frequency and lowest slope segment is resonant nearest the equator. Growth continues. At pulse termination, and characteristic band-limited impulse and end-triggered emissions occur; (*e*) at Lake Mistissini, Quebec, the amplified and dispersed signal is received.

at a particular location, as shown in Figure 4. As each segment of the wave leaves its second order resonance region, the amplified output from that segment becomes the input of the next segment, giving rise to a kind of drifting feedback amplifier. The drift speed along $\vec{B}_0$ increases with the curvature d^2f/dt^2. In terms of the resonant electrons, the length of the interaction region for a particular electron may be significantly reduced with respect to a CW signal on the equator. At the same time the *wave* interaction region is extended to a length defined by the distance along the field line between the second order resonances corresponding to the maximum and the minimum values of df/dt. Thus the resulting expansion along the z axis of the wave interaction region compensates in part for the reduced duration of the wave train. The result is a combination of convective and non-convective growth in which the actual time of growth may be much greater than the duration of the signal. We suggest that this process can account for the high apparent growth rates observed on natural as well at simulated nose whistlers.

Calculations using a model magnetosphere [*Carlson et al.*, 1985] and the NOWS trace of Figure 2 show that the second order resonance locus extends between $z \approx$ 6600 km and $z \approx 29400$ km from the equator at L=4.5. Although the wave train is only 110 ms long, the time of propagation through this region is $\approx$ 620 ms, giving an effective average growth rate as measured in the frame of the traveling wave of only 45 dB/s.

3. Discussion

An important aspect of the second order resonance model described above is that growth is not limited to the region near the equator, but may occur anywhere along the field line as long as the necessary resonant electron distribution exists. Electron pitch angle scattering that results from the interactions would also be enhanced at locations far from the magnetic equator. The location of second order resonance for signals with constant df/dt has been called the "phase equator" [*Helliwell and Inan*, 1982] since this is where the second spatial derivative of the phase between the wave field vectors and the electron's perpendicular velocity is zero. For CW signals the phase equator coincides with the magnetic equator [*Chang et al.*, 1983].

Since this model of the growth of NOWS signals is not limited to the equatorial regions it seems possible that significant growth and associated particle scattering may occur on open field lines extending out to the tail of the magnetosphere. Whistler waves of appropriate frequencies might even reach the earth's moon at times when it is in the tail of the magnetosphere. In that case some of the wave energy could be reflected from the moon's surface back along the same path, to be received at the Earth. Any discontinuities in refractive index, such as might be associated with magnetic field line reconnection, could also scatter energy back to the earth, perhaps of sufficient intensity to permit remote sensing from Earth of irregularities in the geomagnetic tail. We note, however, that because whistler-mode propagation cuts off for $f > f_H$, the sounding frequency must be less than f_H everywhere along the path. We estimate that the wave frequency required for such sounding would be of the order of 200 Hz, about an order of magnitude lower than the frequencies usually employed at Siple Station. Since lightning is known to excite whistlers at such frequencies (as deduced from low altitude satellite observations), it would be interesting to look for whistlers on open field lines, using VLF receivers on future space missions that encounter the geomagnetic tail.

The NOWS experiment described here provides new support for the concept of second order resonance, which has been a central feature of explanations of the various manifestations of the coherent wave instability, underlining the importance of coherence between waves and particles for the growth of whistler-mode signals and the triggering of self-excited narrowband emissions. Enhanced wave-induced precipitation fluxes of energetic particles might also be expected due to the observed rapid growth and frequent triggering of emissions by NOWS clusters which increases the average wave energy (Figure 3). Thus we may expect that frequency-time curvature (d^2f/dt^2) will play an important role in future controlled experiments on wave-particle interactions.

References

Carlson, C. R., R. A. Helliwell, and D. L. Carpenter, Variable frequency VLF signals in the magnetosphere: associated phenomena and plasma diagnostics, *J. Geophys. Res.*, *90*, 1507, 1985.

Chang, H. C., U. S. Inan, and T. F. Bell, Energetic electron precipitation due to gyroresonant interactions in the magnetosphere involving coherent VLF waves with slowly varying frequency, *J. Geophys. Res.*, *88*, 7037, 1983.

Helliwell, R. A., *Whistlers and Related Ionospheric Phenomena*, Stanford Univeristy Press, Stanford, Calif., 1965.

Helliwell, R.A., A theory of discrete VLF emissions from the magnetosphere, *J. Geophys. Res.*, *72*, 4773, 1967.

Helliwell, R. A., Intensity of discrete VLF emissions, *Particles and Field in the Magnetosphere*, B. M. McCormac (ed), 272, D. Reidel, Dordrecht, Amsterdam, 1970.

Helliwell, R. A., D. L. Carpenter, and T. R. Miller, Power threshold for growth of coherent VLF signals in the magnetosphere, *J. Geophys. Res.*, *85*, 3360, 1980.

Helliwell, R. A., and U. S. Inan, VLF wave growth and discrete emission triggering in the magnetosphere: a feedback model, *J. Geophys. Res.*, *87*, 3537, 1982.

Helliwell, R. A., VLF wave stimulation experiments in the magnetosphere from Siple Station, Antarctica, *Rev. Geophys.*, *26*, 551, 1988.

Inan, U. S., M. Walt, H. D. Voss, and W. L. Imhof, Energy spectra and pitch angle distributions of lightning-induced electron precipitation: analysis of an event observed on the S81-1 (SEEP) Satellite, *J. Geophys. Res.*, *94*, 1379, 1989.

R. A. Helliwell, T. Mielke, and U. S. Inan, STAR Laboratory, Stanford University, Stanford, CA 94305

(Received: January 8, 1990;
Accepted: January 31, 1990)